

Moments of nuclear and nucleon structure functions at low Q^2 and the momentum sum rule

I. Niculescu,¹ J. Arrington,² R. Ent,³ and C. E. Keppel^{3,4}

¹*James Madison University, Harrisonburg, VA 22807, USA*

²*Physics Division, Argonne National Laboratory, Argonne, IL 60439, USA*

³*Thomas Jefferson National Accelerator Facility, Newport News, VA 23602, USA*

⁴*Hampton University, Hampton VA 23668, USA*

(Dated: March 24, 2021)

New nuclear structure function data from Jefferson Lab covering the higher x and lower Q^2 regime make it possible to extract the higher order F_2 moments for iron and deuterium at low four-momentum transfer squared Q^2 . These moments allow for an experimental investigation of the nuclear momentum sum rule and a direct comparison of the non-singlet nucleon moment with Lattice QCD results.

PACS numbers: 13.60.Hb, 12.38.Qk, 25.30.Fj

I. INTRODUCTION

Nuclear effects in lepton-nucleus scattering have been extensively studied, both experimentally and theoretically, over the last few decades. For recent reviews, see Refs. [1, 2]. The body of available data provides clearcut evidence that the nucleus can not be simply described as a collection of nucleons on mass shell. For example, the study of nuclear structure functions led to the discovery of the “EMC effect” where it was found that the quark distribution inside the nucleus differs from that of a free nucleon. The availability of experimental information on the Q^2 dependence of the moments of the nuclear structure function $F_2^A(x, Q^2)$ has stimulated theoretical analyses of meson exchange contributions and off-shell effects in nuclei, sometimes showing sizeable deviations from predictions of simple convolution models [3, 4, 5, 6]. In this discussion, A is the mass number, Q^2 is the four-momentum transfer squared in the lepton-nucleon inclusive scattering process, and x is the Bjorken scaling variable, with $0 < x < 1$ for the proton, $0 < x < M_A/M_p \approx A$ for a nucleus.

Previous nuclear structure function moment analyses have relied on moment data extracted from several experiments carried out at CERN [7, 8] and SLAC [9, 10] using ^{56}Fe and ^2H targets. The experimental values of Cornwall–Norton moments, $M_n(A, Q^2)$, require precision measurements of structure functions covering large intervals of x , Q^2 , and A , since:

$$M_n(A, Q^2) = \int_0^A dx F_2^A(x, Q^2) x^{n-2}. \quad (1)$$

Here, n is an integer defining the order of the moments. We note that the $n = 2$ moment can be related to the familiar momentum sum rule, which must be less than unity for the nucleon. Asymptotically, QCD predicts the fraction of the nucleon momentum carried by the quarks to be $(1 + 16/3f)^{-1}$, where f is the number of quark flavors [11].

Until recently, the set of experimental data at large

x was rather poor, and thus the evaluation of the moments was correspondingly imprecise, especially for large n . Typically, data were obtained in the deep inelastic scattering regime at moderate to small values of x and larger values of Q^2 . One can see immediately from Eq. 1 that, as n increases, larger x data will increasingly dominate the moments. Additionally, at lower values of Q^2 , the structure function is larger in the higher x region and dominates even the lower order moments. Moreover, nuclear structure effects are expected to show up most clearly at large values of x [12].

Recently, data have become available from new experiments at Jefferson Lab which cover higher x and lower Q^2 [13, 14, 15, 16], complementing the previous data set. These new data make it possible to accurately extract the moderate and lower Q^2 moments, and moments to higher orders. We report here results from a new extraction of the F_2 structure function moments for iron and deuterium and compare to proton data.

II. EXPERIMENT

Sample spectra used for the extraction of the moments are shown in Fig. 1 for deuterium at $Q^2 = 4.5$ and iron at 5 GeV^2 . As noted above, the calculation of the moment of a structure function requires data covering the whole range in x from 0 to $\approx A$ at a fixed Q^2 . The structure function data used in this analysis were obtained in experiments at SLAC [17, 18], CERN [8, 19], Fermilab [20, 21] and JLab [13, 14, 15, 16]. The Q^2 values where the best coverage in x was available were selected. In some cases, the data were obtained not at exactly the same Q^2 value. In these cases, a small range in Q^2 , varying from 0.01 GeV^2 at low Q^2 to 0.5 GeV^2 at high Q^2 was utilized. The variations of the structure function over such ranges were smaller than 2%.

As illustrated in Fig. 1, the data sets still do not cover the full range in x , some extrapolations were necessary. Between data sets, two methods were utilized,

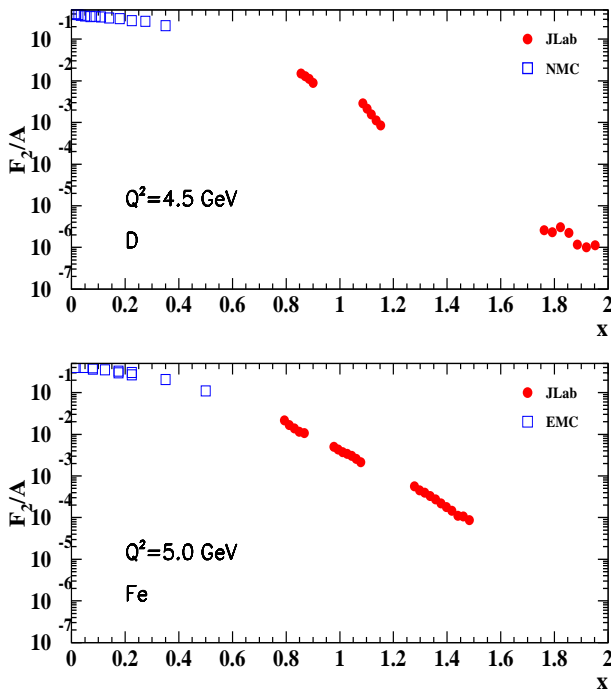


FIG. 1: (Color online) Example structure function data for deuterium (top) and iron (bottom) at $Q^2 = 4.5 \text{ GeV}^2$ and 5 GeV^2 , respectively.

a spline fit and a simple linear extrapolation. Moments obtained in such cases agreed within 2%. To extrapolate to $x \rightarrow 0$ a parameterization from NMC [22] was used for $Q^2 > 2 \text{ GeV}^2$ and a linear extrapolation was used for lower Q^2 data. The uncertainty introduced by this extrapolation becomes negligible for higher order moments. The extrapolation to $x \rightarrow A$, while negligible for $n = 2$, becomes important for the higher moments. The data used in this region were obtained at SLAC and JLab and the coverage in x is sufficient for most Q^2 and n values. The uncertainty in the moments due to the extrapolation to $x = A$ is less than 1% for $n = 2$, around 3% for $n = 4$, up to 6% for $n = 6$, and up to 20% for $n = 8$. The highest x quasielastic and elastic contributions, important for low Q^2 , were calculated according to [23, 24] and added to the moments.

In the near future, the extrapolations to $x \rightarrow 0$ and $x \rightarrow A$ can be improved with new data coming from Jefferson Lab experiments [25, 26, 27, 28, 29, 30, 31]. These experiments have already acquired data and results will become available over the next few years. These newer data will allow for moments to be obtained over an expanded range in Q^2 , and for several additional nuclei, including ^3He and ^4He .

III. RESULTS

Tables I and II show the Cornwall–Norton moments for deuterium and iron. The uncertainties include pub-

Q^2 (GeV^2)	$n = 2$	$n = 4$	$n = 6$	$n = 8$
0.05	.481±.481	.807±.400	2.3618±.2362	8.5266±.8527
0.10	.407±.204	.479±.120	1.0533±.0105	3.3723±.3372
0.20	.320±.080	.284±.034	0.3946±.0395	0.7653±.0765
0.45	.296±.021	.193±.019	0.2163±.0216	0.2968±.0359
0.80	.220±.011	.092±.005	0.0844±.0060	0.0961±.0103
1.50	.180±.009	.040±.003	0.0261±.0020	0.0235±.0033
2.40	.169±.008	.028±.001	0.0165±.0010	0.0156±.0008
3.20	.162±.008	.021±.001	0.0091±.0005	0.0065±.0003
4.50	.165±.008	.016±.001	0.0056±.0003	0.0039±.0002
5.00	.161±.008	.017±.001	0.0052±.0003	0.0030±.0002
7.00	.163±.008	.016±.001	0.0038±.0002	0.0015±.0001

TABLE I: Moments of the F_2 structure function per nucleon for the deuteron.

lished experimental uncertainties on the structure functions, the uncertainties due to the finite Q^2 range of the data and interpolation procedures, extrapolations to low and high x , and the uncertainties in estimating nuclear elastic and quasielastic contributions. The combined uncertainties are typically 5%, except for low Q^2 values where the uncertainty in the quasielastic become very large, especially for $n = 2$. At low Q^2 , the higher moments become increasingly dominated by the nuclear elastic contribution, which is known to better than 5%. For the iron $n = 6$ and $n = 8$ moments, the intermediate Q^2 values have large contributions from the poorly known quasielastic contributions at extremely large x values, and so these moments are not included.

There are indications that two-photon exchange corrections to the electron–nucleon elastic cross section might impact the extracted moments [32]. These corrections appear to be $\lesssim 6\%$ for elastic e - p scattering ($\lesssim 3\%$ for e - n [33]), peaking at large scattering angles. For the data included in this analysis, we expect that two-photon exchange will contribute at most 2% to the moments, typically much less. This is small compared to the experimental uncertainties, and these effects should partially cancel when comparing different nuclei.

The lower n moments display a very shallow to negligible Q^2 dependence. In the Operator Product Expansion (OPE), higher twist effects (interactions between the struck quark and other quarks in the electron–nucleon scattering process) are expected to manifest a $1/Q^2$ dependence in the moment. This is not observed in the data, which is somewhat surprising at these low Q^2 values where such effects could be large. The asymptotic behavior of the second moment is ultimately governed by the energy–momentum tensor in the OPE and, thus, has no Q^2 dependence, as in the quark–parton model [11]. Even at the low Q^2 values studied here, the moments display this quark–parton model behavior over most of the Q^2 range. The lower Q^2 moments are dominated by high x

Q^2 (GeV ²)	$n = 2$	$n = 4$	$n = 6$	$n = 8$
0.05	.203±.203	204±10	(6.4±.32)×10 ⁵	(2.0±.1)×10 ⁹
0.10	.207±.100	5.74±.289	(1.77±.09)×10 ⁴	(5.6±.28)×10 ⁷
0.25	.277±.069	.273±.137	2.763±1.242	6600±330
0.40	.265±.027	.273±.041	—	—
1.00	.209±.010	.095±.005	0.276±0.044	—
1.90	.166±.008	.034±.002	0.0270±0.0015	.0447±.0058
2.90	.174±.009	.018±.001	0.0114±0.0010	.0146±.0063
5.00	.158±.008	.015±.001	0.0050±0.0004	.0032±.0006
6.00	.164±.008	.016±.001	0.0038±0.0002	.0020±.0004

TABLE II: Moments of the F_2 structure function per nucleon for iron.

resonance regime. Hence, this observation is yet another striking manifestation of quark–hadron duality [34].

The higher n moments, on the other hand, do display an increased Q^2 dependence. These data may therefore be used for precision higher twist extractions. However, the higher n moments are increasingly dominated by the high x , including the elastic and quasi–elastic regimes, where the x and Q^2 dependences are less well understood in terms of the OPE.

If nuclear effects are small, the moments for iron can also be constructed by adding the proton and neutron contributions, extracted from proton [35] and deuteron data. To investigate how well this simplified approach works, the following simple formula was employed:

$$M_n(Fe) = Z \times M_n(p) + (A - Z) \times M_n(n), \quad (2)$$

where $M_n(n)$ is taken to be $M_n(d) - M_n(p)$. Here, $M_n(p)$, $M_n(n)$, and $M_n(d)$ refer to the n th moment of the proton, neutron, and deuteron, respectively, and Z is the atomic number of iron. This is equivalent to extracting the iron data as 28 deuterons with a small neutron excess contribution. Simple Fermi motion should not yield a significant nuclear dependence in the M_2 moment, and off-shell effects have been studied [5, 6] and are also expected to be small for the lowest moment, and on the order of 10% for moments up to $n = 5$ [5].

This procedure is illustrated in Fig. 2 for the second moment, M_2 . The iron data are shown as squares, deuteron data as full circles, proton data as stars. The red dashed lines describing the deuteron and the proton moments are simple fits to the proton and deuteron data, which are then used to calculate the neutron moment, $M_2(d) - M_2(p)$, and the iron moment as 26 protons and 30 neutrons, as described in Eq. 2. No additional correction was made for nuclear effects or the non–isoscality of the target. The neutron and iron moments thus calculated are shown as blue dashed lines in the figure, while the hollow circles show the neutron moments taken directly from the difference of deuteron and proton moments. For $Q^2 > 4$ GeV², the ratio of $M_2(Fe)/M_2(D)$, normalized

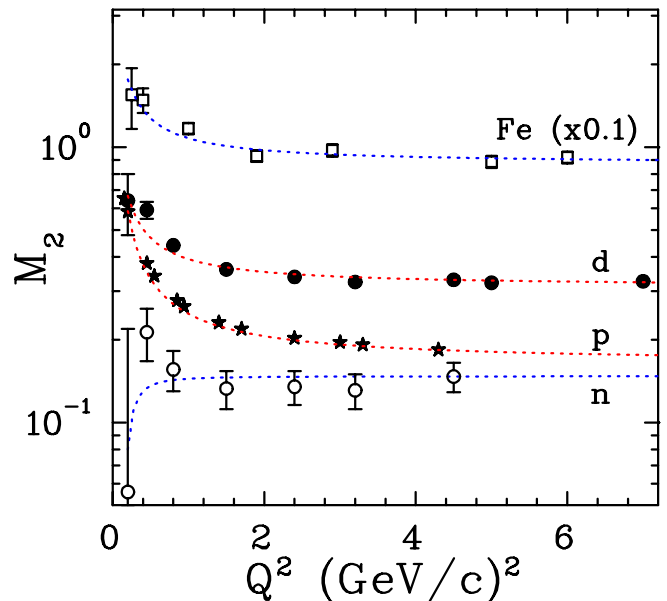


FIG. 2: (Color online) The second moment of F_2 for proton (stars), deuteron (full circles), and iron (squares). The hollow circles are the neutron moments taken from the difference of deuteron and proton. The red dashed lines are fits to the deuteron and proton moments, and the blue dashed lines are the neutron and iron moments extracted from these fits using the procedure described in the text.

to the number of nucleons, is 0.99 ± 0.05 , consistent with the value 0.96 [36], from a calculation based on Ref. [5].

The ratios of the measured moments for iron compared to the moments taken from the deuteron and proton moments are shown in Fig. 3. It can be seen that these two methods yield the same results within the uncertainty. Combining all of the values yields a deviation of $(0.9 \pm 2.2)\%$, or $(0.5 \pm 2.9)\%$ if we consider only $Q^2 > 2.5$ GeV². This result contradicts interpretations of the EMC effect that predict significant modification to the the *total* quark momentum distribution in nuclei. However, it is consistent with other interpretations where the total quark momentum is conserved [2, 37]. Here, the data indicate that the integrated iron nucleus can be described well as simply being composed of free deuterons, with a minimal correction for neutron excess in $26p + 30n$. It seems the EMC effect is a redistribution of quark momentum without any additional momentum added by the nuclear environment outside of whatever is already present in the deuteron.

One can also connect the nuclear dependence of the quark distributions to the coordinate space parton distributions [38, 39]. The A dependence of the $n = 2$ moment is then related to the A dependence of the light cone distributions at short distance. The fact that the data indicate extremely small nuclear effects is consistent with the result that the A dependence for distances less than the inter-nucleon spacing is surprisingly small ($< 2\%$), due to cancellation between the shadowing, anti-

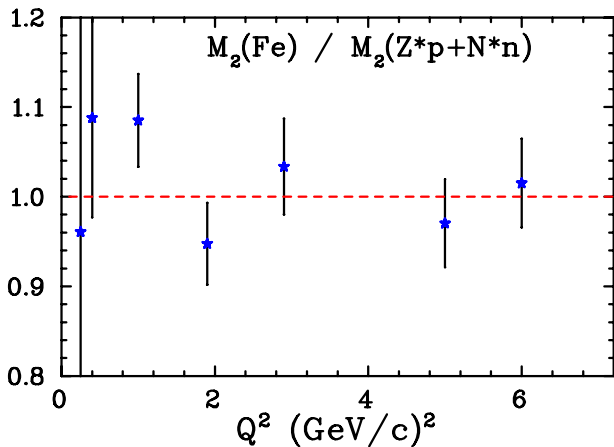


FIG. 3: (Color online) The ratio of the QCD moments for iron calculated using iron data to the moments constructed using deuterium and proton data shown as a function of Q^2 .

shadowing, and EMC regions [38].

We note, further, that the redistribution can be quite large, locally. In the structure functions at fixed (x, Q^2) values, there are drastic differences in the nucleon and in nuclei. For instance, resonance structure can be observed in the Δ resonance region in deuterium but not at all in iron. However, the effect of this redistribution is smaller in nuclei, such that the resonance region structure function nearly reproduces the DIS structure function in nuclei [14, 18], and the ratios of the nuclear structure function in the resonance region reproduce the observed EMC effect with high precision [40].

West points out the need to reconcile the difference between the fundamental asymptotic QCD sum rule,

$$\int_0^A \left(\frac{1}{A} F_2^A - \frac{1}{2} F_2^D \right) dx = 0, \quad (3)$$

based on energy-momentum conservation, and the nominal observation of the EMC effect that the nuclear structure function is not simply A times that of a nucleon [11]. The new data presented here (Fig. 3) indicate agreement with this sum rule already at the low Q^2 values here observed. As a quantitative example, the integral in Eq. 3 becomes of the order of 4×10^{-3} compared to individual moments of ~ 0.2 at $Q^2 = 2.9 \text{ GeV}^2$.

The moments of the structure function F_2 can be determined theoretically on the lattice [41, 42, 43]. While contributions from disconnected diagrams [41] make it more difficult to calculate the separate proton and neutron moments on the lattice, these contributions cancel in the non-singlet combination $M_n(p) - M_n(n)$. To compare our results with lattice calculations we extracted the difference between the proton and neutron moments for $n=2$ and $n=4$. We assume that the deuteron moment is equal to the sum of proton and neutron, and then determining the $p - n$ moment from the proton [35] and deuteron moments, taking $M_n(p-n) = 2M_n(p) - M_n(d)$. Because the proton and deuteron moments are sometimes

	This work $Q^2 \approx 4 \text{ GeV}^2$	Detmold <i>et al.</i> [42]	Dolgov <i>et al.</i> [41]	Gockeler <i>et al.</i> [43]
$n = 2$	0.049(17)	0.059(8)	0.269	0.245
$n = 4$	0.015(03)	0.008(3)	0.078	0.059

TABLE III: Moments of the F_2 structure function for the difference $p - n$. Experimental results for $Q^2 \approx 4 \text{ GeV}^2$ from the present work are compared to lattice calculations at 4 GeV^2 .

extracted at slightly different Q^2 values, we combine our extracted deuteron moments with the nearest proton moments, scaling the proton to the correct Q^2 value using the Q^2 dependence of the simple fit shown in Fig. 2. The extracted values for the M_2 and M_4 moments for $p - n$ are independent of Q^2 above 2 GeV^2 . The experimental results shown in Table III for $Q^2 \approx 4 \text{ GeV}^2$ come from combining the extracted values at $Q^2 = 3.2$ and 4.5 GeV^2 , and are compared to lattice calculation at $Q^2 = 4 \text{ GeV}^2$. Because the proton and neutron $n = 2$ moments are comparable in size, there is a large cancellation in the difference which leads to the large relative uncertainty.

The $n = 2$ moment from Detmold *et al.* [42] is in excellent agreement with the measured data. For $n = 4$, the small discrepancy between the lattice calculation and our experimental result could be due to higher twist effects, which are not included in the lattice result, although the Q^2 dependence of the moments does not indicate that these are large. In addition, no nuclear effects were taken into consideration when extracting the neutron moment from deuterium data. These effects seem to be small when averaged over the entire x range but they might still have some non-negligible contribution. It should also be noted that there are still open issues for lattice calculations, such as chiral extrapolation, volume dependence, or renormalization. To demonstrate this, we also show the results of Dolgov *et al.* [41], and Gockeler *et al.* [43]. The main difference between the lattice calculations presented here is the chiral extrapolations used. In Ref. [41], the lattice results are extrapolated linearly to the physical limit, while in Ref. [42], the extrapolation includes the correct chiral behavior from chiral effective theory.

We note that comparisons between lattice and nominal data formed from pdf-based fits have been performed previously [42]. We stress that such fits do not adequately account for the large x regime where they are unconstrained by data. Moreover, substantial uncertainties exist in the down quark distribution, $d(x)$, associated with assumptions utilized in extracting neutron results from deuteron data, as well as the unknown behavior of d/u as $x \rightarrow 1$.

IV. CONCLUSIONS

In conclusion, we utilized inclusive electron–nucleus scattering data to obtain nuclear structure function moments for iron and deuterium. The new data are particularly important for moment calculations at low Q^2 , where there was a paucity of previous data. Moreover, at low Q^2 and higher n , the need for large x data increases as this regime comes to dominate the moments.

Negligible Q^2 dependence is observed in the lower order moments, indicating agreement with asymptotic predictions and minimal higher twist effects. This is surprising, given that the data extend to quite low Q^2 values.

The $n = 2$ moment, related to the momentum sum rule, is here presented for both iron and deuterium. Additionally, a neutron momentum was formed by subtracting existing proton data from the deuterium data. The measured iron moments were found to agree with mo-

ments simply constructed from these neutrons and protons. This observation has interesting implications for interpretations of the EMC effect.

Finally, these neutron and proton moment data allow for comparison with lattice QCD calculations. The extracted non-singlet moments provide the first direct comparison to lattice calculations of the non-singlet moments and the results are in good agreement with the calculation of Ref. [42].

Acknowledgments

This work was supported in part by DOE Grants W-31-109-ENG-38 and DE-FG02-95ER40901, and NSF Grants 0099540 and 0245045. We thank Wally Melnitchouk for useful discussions.

-
- [1] M. Arneodo, *Phys. Rept.* **240**, 301 (1994).
 - [2] D. F. Geesaman, K. Saito, and A. W. Thomas, *Ann. Rev. Nucl. Sci.* **45**, 337 (1995).
 - [3] O. B. S. Fantoni and G. I. Lykasov, *Nucl. Phys.* **A699**, 140 (2002).
 - [4] O. B. S. Fantoni and G. I. Lykasov, *Phys. Lett. B* **502**, 69 (2001).
 - [5] C. D. Cothran, D. B. Day, and S. Liuti, *Phys. Lett. B* **421**, 46 (1998).
 - [6] W. Melnitchouk, A. W. Schreiber, and A. W. Thomas, *Phys. Lett. B* **335**, 11 (1994).
 - [7] J. J. Aubert et al. (European Muon Collaboration), *Nucl. Phys.* **B293**, 740 (1987).
 - [8] J. J. Aubert et al. (European Muon Collaboration), *Nucl. Phys.* **B272**, 158 (1986).
 - [9] J. Gomez et al., *Phys. Rev. D* **49**, 4348 (1994).
 - [10] J. Arrington et al., *Phys. Rev. C* **53**, 2248 (1996).
 - [11] G. B. West, *Phys. Rev. Lett.* **54**, 2576 (1985).
 - [12] L. P. Kaptari, A. Y. Umnikov, and B. Kampfer, *Phys. Rev. D* **47**, 3804 (1993).
 - [13] J. Arrington et al., *Phys. Rev. Lett.* **82**, 2056 (1999).
 - [14] J. Arrington et al., *Phys. Rev. C* **64**, 014602 (2001).
 - [15] I. Niculescu et al., *Phys. Rev. Lett.* **85**, 1182 (2000).
 - [16] I. Niculescu et al., *Phys. Rev. Lett.* **85**, 1186 (2000).
 - [17] S. Dasu et al., *Phys. Rev. D* **49**, 5641 (1994).
 - [18] B. W. Filippone et al., *Phys. Rev. C* **45**, 1582 (1992).
 - [19] J. P. Berge et al., *Z. Phys.* **C49**, 187 (1991).
 - [20] E. Oltman et al., *Z. Phys.* **C53**, 51 (1992).
 - [21] M. R. Adams et al. (E665), *Phys. Rev. D* **54**, 3006 (1996).
 - [22] M. Arneodo et al. (New Muon Collaboration), *Phys. Lett. B* **364**, 107 (1995).
 - [23] C. W. De Jager, H. De Vries, and C. De Vries, *Atom. Data Nucl. Data Tabl.* **14**, 479 (1974).
 - [24] M. M. Sargsian, Jefferson Lab CLAS-NOTE 90-007, http://www.jlab.org/Hall-B/notes/clas_notes90.html.
 - [25] A. Bruell, C. E. Keppel, J. Dunne, et al., Jefferson Lab experiment E99-118.
 - [26] C. E. Keppel, I. Niculescu, et al., Jefferson Lab experiment E00-002.
 - [27] C. E. Keppel et al., Jefferson Lab experiment E00-116.
 - [28] J. Arrington, D. Day, A. Lung, B. Filippone, et al., Jefferson Lab experiment E02-019.
 - [29] M. E. Christy, C. E. Keppel, et al., Jefferson Lab experiment E02-109.
 - [30] J. Arrington, D. Gaskell, et al., Jefferson Lab experiment E03-103.
 - [31] A. Bodek, C. E. Keppel, et al., Jefferson Lab experiment E04-001.
 - [32] J. Arrington, *Phys. Rev. C* **69**, 022201(R) (2004).
 - [33] P. G. Blunden, W. Melnitchouk, and J. A. Tjon (2005), nucl-th/0506039.
 - [34] W. Melnitchouk, R. Ent, and C. Keppel, *Phys. Rep.* **406**, 129 (2005).
 - [35] C. S. Armstrong et al., *Phys. Rev. D* **63**, 094008 (2001).
 - [36] S. Liuti, private communication.
 - [37] K. Saito and K. Tsushima, private communication (2005).
 - [38] P. Hoyer and M. Vanttinen, *Z. Phys.* **C74**, 113 (1997).
 - [39] M. Vanttinen, G. Piller, L. Mankiewicz, W. Weise, and K. J. Eskola, *Eur. Phys. J.* **A3**, 351 (1998).
 - [40] J. Arrington, R. Ent, C. E. Keppel, J. Mammei, and I. Niculescu (2003), nucl-ex/0307012.
 - [41] D. Dolgov et al. (LHPC), *Phys. Rev. D* **66**, 034506 (2002).
 - [42] W. Detmold, W. Melnitchouk, and A. W. Thomas, *Phys. Rev. D* **66**, 054501 (2002).
 - [43] M. Gockeler et al. (2004), hep-ph/0410187.